Title
THE CRYOGENIC MECHANICAL PROPERTIES AND THE INTERGRANULAR BRITTLENESS IN Fe-12%MN-(0.2%Ti) FERRITIC ALLOY SYSTEM

Permalink
https://escholarship.org/uc/item/74b3j0nh

Author
Hwang, S.K.

Publication Date
1978-06-01

Submitted to Journal of
Korean Institute of Metals

LBL-8018
Preprint

THE CRYOGENIC MECHANICAL PROPERTIES AND THE INTERGRANULAR BRITTLENESS IN Fe-12%Mn-(0.2%Ti) FERRITIC ALLOY SYSTEM

S. K. Hwang

June 1978

Prepared for the National Aeronautics and Space
Administration under Contract NASA-NGR-05-003-562 and
the U. S. Department of Energy under
Contract W-7405-ENG-48

THE CRYOGENIC MECHANICAL PROPERTIES AND THE INTERGRANULAR BRITTLENESS IN Fe-12%Mn-(0.2%Ti) FERRITIC ALLOY SYSTEM

S. K. Hwang

Department of Materials Science and Mineral Engineering and,
Materials and Molecular Research Division, Lawrence Berkeley Laboratory
University of California, Berkeley, California 94720

ABSTRACT

An investigation toward a nickel-free ferritic cryogenic Fe-12%Mn-(0.2%Ti) alloy steel was made, and the metallurgical processing techniques which improve the cryogenic mechanical properties are summarized. Retained austenite produced by a heat treatment within the two-phase $(\alpha + \gamma)$ region was found to be effective in suppressing cryogenic brittleness. The inherent intergranular weakness of this alloy was also studied by employing Auger electron spectroscopy and other techniques. The cause of the intergranular brittleness is discussed and a method for its prevention is suggested.

INTRODUCTION

The demand for storage and transportation materials for liquified natural gas is rapidly increasing. The materials for this application must have a suitable combination of strength and toughness at subzero temperatures. A commercial 9Ni steel meets the requirements satisfactorily.(1) However, the cost of Ni is high, which stimulates researches on lower nickel(2) or even nickel-free(3) cryogenic alloys.

Among the iron-base alloys, the Fe-Mn system is a ptoential candidate for the nickel-free cryogenic steel. The composition range of specific interest is 8∿12%.* The low temperature transformation product in this range is mainly α' (bcc) martensite, which ensures an adequate cryogenic strength. Particularly an Fe-12Mn alloy has a promising combination of strength and toughness. Alloys with higher Mn concentration (>15%Mn) have either stabilized γ (fcc) or ε (hcp) or mixed $\gamma + \varepsilon$ structures. They retain relatively high toughness but have low strength at cryogenic temperatures.

Holden et al. (4) and Roberts (5) surveyed the transformation behavior of Fe-2∿40%Mn and Fe-0∿9%Mn alloys respectively, while others (6,7) studied their ductile-to-brittle transition behavior. Hwang and Morris (8) identified thermal/mechanical processing techniques to improve the cryogenic mechanical properties of Fe-8%Mn and Fe-12%Mn alloys.

The search toward a simpler, economical method to improve the mechanical properties is currently underway at the Lawrence Berkeley Laboratory (LBL). This search is proceeding through the investigation of fundamental aspects of fracture characteristics at low temperature. Intergranular fracture in Fe-12%Mn is an example. The present paper aims at: (1) summarizing the effect of processing techniques developed at LBL, (2) analyzing the

---

*Weight percent unless otherwise specified.

intergranular fracture in an Fe-12%Mn alloy and suggesting a way for its prevention.

EXPERIMENTAL PROCEDURE

10 kg ingots of Fe-12%Mn-0.2%Ti alloys were vacuum induction melted. The cast ingots were homogenized at 1200°C for 24 hours under argon atmosphere. Then they were forged into 1.3 cm and 2.6 cm thick plates from which specimens were made. Chemical analysis of a test specimen showed 11.9%Mn, 0.16%Ti, 0.001%C, 0.028%O, 0.007%S and 0.007%P.

ASTM full-size V-notched specimens were used for Charpy impact tests. The specimens for tensile tests were subsized and cylindrical with 1.3 cm gage length and 0.7 cm gage diameter. Plane strain fracture toughness (K_{IC}) values were obtained from compact tension specimens with 2.5cm thickness.

The microstructures were examined by optical and transmission electron microscopy (TEM). The volume percent of different phases was determined by x-ray diffraction. The fracture surfaces were examined under the scanning electron microscope (SEM). The composition of the fracture surfaces was analyzed by scanning Auger electron spectroscopy (AES). To obtain a fresh surface the specimens were fractured inside a vacuum chamber maintained at $10^{-9} \sim 10^{-10}$ torr pressure.

EXPERIMENTAL RESULTS AND DISCUSSION

1. Properties of as-austenized Fe-12%Mn-0.2%Ti alloy

According to Holden et al.(4) the transformation products of as-cooled low carbon Fe-Mn alloys are as follows:

(i) 0∿2%Mn: equiaxed or massive ferrites
(ii) 2∿6%Mn: upper bainite

(iii) 6∿10%Mn: lath martensite (α', bcc structure)
(iv) 10∿15%Mn: α' + epsilon (ε, hcp)
(v) 15∿28%Mn: ε + austenite (γ, fcc)
(vi) 28∿37%Mn: γ.

FIG. 1

In the present study the austenitizing treatment was done at 900°C for 2 hours followed by water quenching. The microstructures of the as-austenitized Fe-12%Mn-0.2%Ti are shown in Fig. 1. The α' martensite laths are highly dislocated. The individual lathes within a packet is divided into blocks. The lath boundaries were often covered with thin ε platelets as shown in Fig. 1(b), which is a dark field TEM micrograph. The volume percent of the ε martensite measured by x-ray diffraction was approximately 15% at -196°C.

Table I

The mechanical properties of Fe-12%Mn-0.2%Ti alloy are given in Table I. The alloy has high yield and ultimate tensile stresses at -196°C. However, as shown in Fig. 2, the as-austenitized specimen undergoes a sharp ductile-to-brittle transition under impact condition at approximately -50°C. The initial properties, especially the impact toughness can be improved by the thermal/mechanical treatments described below.

2. Effect of thermal/mechanical treatments on the cryogenic mechanical properties.

The impact toughness of α' martensitic Fe-Ni steels is improved by a heat treatment within the $\alpha + \gamma$ range of the equilibrium phase diagram.(9-10) When heated the metastable α' martensite decomposes to yield equilibrium γ and α. The reverted γ phase is enriched with alloying elements thus becoming stabilized. This γ phase may be found untransformed at subzero temperature, and is called "retained γ". Several researchers(9-12) have attributed the improvement of impact toughness in the Fe-Ni alloys to the retained γ.

Like Fe-Ni, the Fe-Mn system has an $\alpha + \gamma$ which extends to room temperature. Therefore, the $\alpha' \rightarrow \alpha + \gamma$ transformation also occurs in Fe-12Mn. However, the ε martensite in this alloy complicates the reaction. On heating a diffusionless transformation ($\varepsilon \rightarrow \gamma$) occurs over the range of temperatures $240 \sim 350$°C. The γ phase formed in this manner will affect the diffusional $\alpha' \rightarrow \alpha + \gamma$ at higher temperature.

The correlation between retained γ and impact toughness was observed in the tempered Fe-12%Mn-0.2%Ti alloy. A simultaneous increase in the amount of retained γ and in the Charpy impact energy was found after heating at 500°C.(9) Various cryogenic mechanical properties were measured on the alloy heat treated for 8 hours at 500°C. The results are presented in Table I and in Fig. 2. The yield strength at -196°C was slightly increased by the tempering treatment. Concurrently, a significant reduction of the ductile-to-brittle transition temperature occurred.

FIG. 2

The microstructure of a tempered (500°C/120 hrs) specimen is shown in Fig. 3. The apparent extreme directionality of the microstructure is a consequence of an elongated growth of γ along α' lath boundaries. This was presumably caused by the diffusionless transformation $\varepsilon \rightarrow \gamma$ during heating. The reverted γ, decorating lath boundaries at the previous ε sites, serves as preferential growth sites for new γ in the subsequent $\alpha' \rightarrow \alpha + \gamma$ reaction. Therfore, a more uniform distribution of phases can be obtained by destroying the ε. The elimination of ε can be achieved by cold working, which induces an $\varepsilon \rightarrow \alpha'$ transformation by strain.(7) Also, the dislocations created by cold working may act as heterogeneous nucleation sites.

FIG. 3

FIG. 4

The microstructure obtained after a 50% reduction at room temperature followed by annealing at 500°C for 8 hrs is shown in Fig. 4. The uniformity and the fineness of the phases are evident.

FIG. 5

The cryogenic strength and toughness of an Fe-12%Mn-0.2%Ti alloy were significantly enhanced by the cold working and two phase annealing treatment. The properties are shown in Table I and Fig. 2. The increases in the yield strength and the impact shelf energy are particularly noticeable. By varying the annealing temperature it was possible to observe the correlationship between the cryogenic impact energy and the retained γ. A remarkably good correspondence was found between the two, as shown in Fig. 5.

3. Intergranular fracture in Fe-12%Mn alloy

The potential of an Fe-12%Mn alloy system as a nickel-free cryogenic alloy was demonstrated by the mechanical properties obtained after thermomechanical processing. However, the mechanical/thermal treatment may add to the cost of practical production. A more economical processing was sought through investigating the fundamental aspects of the fracture behavior of this alloy. The preliminary results of this investigation are described below.

a. Fracture modes

FIG. 6

Though both have principally an α' martensitic structure, Fe-8%Mn and Fe -12%Mn alloys have quite different fracture modes below their ductile-to- brittle transition temperature. Examples are shown in Fig. 6. The Fe-8%Mn alloy shows transgranular cleavage with occasional secondary cracks along martensite packet boundaries. In contrast, the Fe-12%Mn fails along prior γ boundaries. The addition of titanium (0.2%) does not affect the fracture mode itself. Above the transition temperature both alloys show ductile void type fracture surface.

Intergranular fracture of the 12Mn steel was observed in specimens as quenched after austenitizing treatment. The fracture was removable by the mechanical/thermal treatments but could not be eliminated by tempering treatments alone. On the other hand the tendency twoard intergranular fracture could be aggravated by a heat treatment at 350°C. After holding for 2 hours at this temperature the transition temperature in Charpy tests was increased by 130°

b. Grain boundary composition

Intergranular fracture in commercial alloy steels is often attributed to impurity segregation.(13-14) The segregation is believed to occur within several atomic layers. A powerful technique to detect the thin layer segregation is Auger electron spectroscopy (AES). Secondary electrons produced by Auger process have a very short escape depth. Therefore, the AES is widely acknowledged as a highly surface sensitive probing technique.(15)

The details of the application of the AES technique are described elsewhere.(16) It is essential to produce the desired fracture surface in a ultra high vacuum ($10^{-9} \sim 10^{-10}$ torr) chamber in which SEM and AES analyzing devices are incorporated. The analyses are carried out on the fresh surface which had not been exposed to air. The spatial resolution depends on the filament and analyzer design. In the present investigation the maximum resolution was 15μm* diameter.

FIG. 7

Auger electron spectra obtained from the grain boundaries of as-quenched and embrittled specimens are shown in Fig. 7(a) and (b) respectively. The as-quenched prior austenite grain boundaries had

---

*A submicron resolution is now commercially available.

essentially the same composition as the bulk. The embrittled (350°C/2 hrs) grain boundaries showed a high Mn concentration, approximately 24%. The effect of the Mn enrichment on the shift of the transition temperature awaits further investigation. However, it is clear that intergranular fracture in the as-quenched 12Mn alloy steel does not require impurity or alloying element segregation.

The possibility of the microstructural change on the prior γ grain boundaries was also examined by TEM. Neither precipitation nor a preferential distribution of a particular phase, e.g., ε, was observed along the grain boundaries. Therefore, any hypothesis based on compositional or microstructural change on the prior γ boundaries fails to explain the intergranular fracture behavior of Fe-12%Mn alloys in the as-quenched condition.

c. Hypothesis and preventive mechanism

On the basis of the previous experimental results, the following hypothesis may be suggested. The fracture stress of the prior γ boundaries, σ_{FGB}, is approximately the same for Fe-8%Mn and Fe-12%Mn alloys. However, the fracture stress for the transgranular crackings, σ_{FC}, is higher in Fe-12%Mn. This is because of the ε phase decorating the lath boundaries inside prior γ grains, as shown in Fig. 1. Being a soft phase, ε blunts and deviates the sharp front of the propagating crack.

FIG. 8

A schematic diagram can be constructed along lines suggested long ago by Davidenko shown in Fig. 8. The ductile-to-brittle transition occurs at a temperature where the lower of σ_{FGB} and σ_{FC} intersects with the matrix yield stress, σ_y. Therefore, $(T_c)_{8Mn} > (T_c)_{2Mn}$, where T_c is the transition temperature. Also, below T_c the fracture mode is transgranular cleavage for Fe-8%Mn and intergranular for Fe-12%Mn alloys.

These are consistent with the experimental observation.

If the above hypothesis holds then a preventive method for the intergranular cracking in 12Mn alloy may be designed. According to Griffith's fracture theory,

$$\sigma_F = \frac{2E\gamma_I}{\pi c} \quad ,$$

where E is Young's modulus, c is the length of edge crack and γ_I is the surface energy created by fracture. In the intergranular fracture case, $\sigma_F = \sigma_{FGB}$ and $\gamma_I = 2\gamma_s - \gamma_b$, where γ_s is the energy of new surfaces and γ_b is the grain boundary energy. Therefore, to increase σ_{FGB} an element can be added which decreases γ_b significantly while not decreasing γ_s too much. Such an element should segregate to the grain boundaries, but will not cause embrittlement. The information on the effects of the alloying elements on the grain boundary properties of some intermediate carbon steels (17) and super alloys (18) may be helpful. However, there is a considerable lack of information on various elements' relative effects on γ_s and γ_b. Therefore, the success of this effort will depend heavily on empirical study backed up by sophisticated analyzing instrumentation.

SUMMARY

The following summarizes the present investigation for a development of a nickel-free ferritic Fe-12%Mn steel:

(1) A two phase ($\alpha + \gamma$) heat treatment is beneficial for the impact toughness.

(2) A cold-working process followed by two phase annealing enhances cryogenic strength and toughness significantly. This result is attributed to the increased amount of retained γ and the fineness of the structure.

(3) The intergranular fracture in the as-quenched condition is not a consequence of the reduced grain boundary fracture stress, σ_{FGB}, due to a chemical or microstructural change on the prior γ boundaries during austenitizing. The fracture stress for the transgranular crackings, σ_{FC}, is rather increased due to the dispersion of the ε phase.

(4) A better alloy composition may be obtained by adding an element which can reduce the grain boundary energy, γ_b, while moderately maintaining the surface energy, γ_s.

ACKNOWLEDGMENT

This work was supported by the Division of Materials Sciences, Office of Basic Energy Sciences, U. S. Department of Energy and carried out at the Materials and Molecular Research Division of the Lawrence Berkeley Laboratory.

The support of the National Aeronautics and Space Administration, Lewis Research Center under Contract No. NASA-NGR-05-003-562 is also gratefully acknowledged.

REFERENCES

1. A. W. Pense and R. D. Stout: "Fracture Toughness and Related Characteristics of the Cryogenic Nickel Steels," Welding and Research Council Bulletin, 205 (1975).
2. S. Nagashima, T. Ooka, S. Sekino, H. Mimura, T. Fujishima, S. Yano, H. Sakurai: Trans. Iron Steel Inst. Japan 11 (1971) 402.
3. V. I. Grigorkin: Metal Sci. Heat Treat. 7 (1969) 568.
4. A. Holden, J. D. Bolton and E. R. Petty: J. Iron Steel Inst. 209 (1971) 721.
5. M. J. Roberts: Met. Trans. 2 (1970) 3287.
6. J. D. Bolton, E. R. Petty and G. B. Allen: Met. Trans. 2 (1971) 2915.
7. M. J. Schanfein, M. J. Yokota, V. F. Zackay, E. R. Parker and J.W. Morris, Jr. ASTM STP 579 (1975) 361.
8. S. K. Hwang: Ph.D. Thesis, U. C. Berkeley 1977.
9. C. W. Marschall, R. F. Heheman and A. R. Troiano: Trans. ASM, 55 (1962) 135.
10. S. K. Hwang, S. Jin and J. W. Morris, Jr., : Met. Trans. A 6 (1975) 2015.
11. S. Jin, S. K. Hwang and J. W. Morris, Jr.,: Met. Trans. A 6A (1975) 1721.
12. H. Haga: Trans. Iron Steel Inst. Japan 13 (1973) 141.
13. C. J. McMahon, Jr.: Proceedings "4th Bolton Landing Conference on Grain Boundaries in Engineering Materials", Editors J. L. Walter, J. H. Westbrook and D. A. Woodford, Claitors (1974) 525.
14. B. D. Powell, H. J. Westbrook, D. M. R. Taplin and H. Mykura: Met. Trans. 4 (1973) 2357.

15. L. A. Harris: J. Appl. Phys. 39 (1968) 1419.

16. D. F. Stein, A. Joshi and R. P. Laforce: Trans. ASM 62 (1969) 776.

17. A. M. Adaii, J. W. Spretnak and R. Speiser: Trans. AIME, J. Metals 203 (1955) 353.

18. R. F. Decker: "Strengthening Mechanisms in Nickel-Base Superalloys", Steel Strengthening Mechanisms Symp. Zurich, Switzerland, 1969, INCO Report A-553.

19. S. K. Hwang, S. Jin and J. W. Morris, Jr.,: Proceedings "4th International Conference on the Strength of Materials and Alloys," Nancy, France 2 (1976) 842.

TABLE I. MECHANICAL PROPERTIES OF Fe-Mn ALLOYS

Composition	Treatment	Test Temp. (°C)	σ_y (MNm^{-2})	σ_{uts} (MNm^{-2})	Uniform Elong. (%)	Total Elong. (%)	Red. in Area (%)	K_{IC} ($MNm^{-3/2}$)
Fe-12Mn-0.2Ti	As-Quenched	25	600	924	6	25	78	-
"	"	-196	889	1351	11	25	54	63
"	500°C/8 hrs	-196	952	1358	18	33	62	70
"	50% reduction +600°C/4 hrs	-196	1179	1503	26	38	66	100

FIGURE CAPTIONS

FIG. 1. Fe-12%Mn-0.2%Ti. As-quenched from austenitizing (900°C/2 hrs). TEM micrographs; (a) Bright field (BF) (b) Dark field (DF) of ε phase.

FIG. 2. Fe-12%Mn-0.2%Ti. Ductile-to-brittle transition behavior of differently processed specimens in Charpy impact tests.(19)

FIG. 3. Fe-12%Mn-0.2%Ti. Two-phase tempered structure (500°C.120 hrs). TEM micrographs; (a) BF (b) DF of retained γ.

FIG. 4. Fe-12%Mn-0.2%Ti. A TEM micrograph of a cold-worked (50%) and two-phase annealed (600°C/4 hrs) specimen.(19) Retained γ shows dark contrast.

FIG. 5. Fe-12%Mn-0.2%Ti. Charpy V-notched impact energy at -196°C (CVN) and the phase constituents of specimens cold-worked (50%) and annealed at various temperatures for 4 hours.(19)

FIG. 6. SEM fractographs of Charpy specimens broken at -196°C. (a) Fe-12%Mn-0.2%Ti (b) Fe-8%Mn. All as-austenitized.

FIG. 7. Auger electron spectra of Fe-12%Mn specimens. (a) As-austenitized. (b) Embrittled. Note higher concentration of Mn in (b).

FIG. 8. A schematic diagram describing different fracture modes and transition temperatures in Fe-12%Mn and Fe-8%Mn alloys.

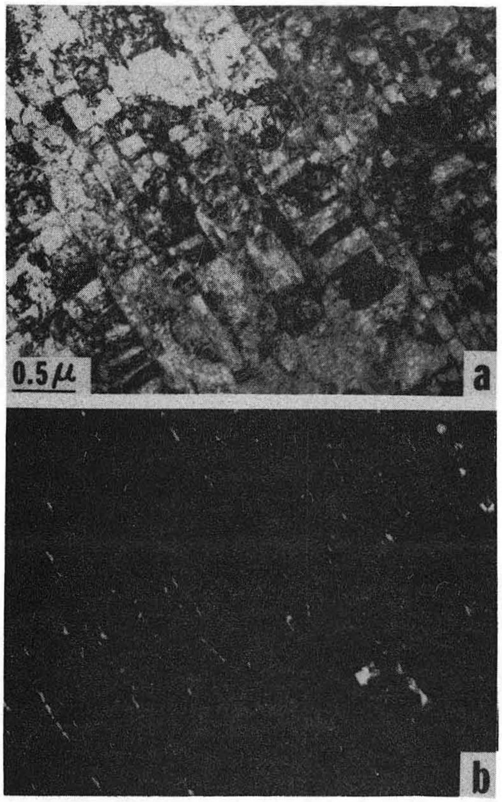

XBB 786-6722

FIG. 1

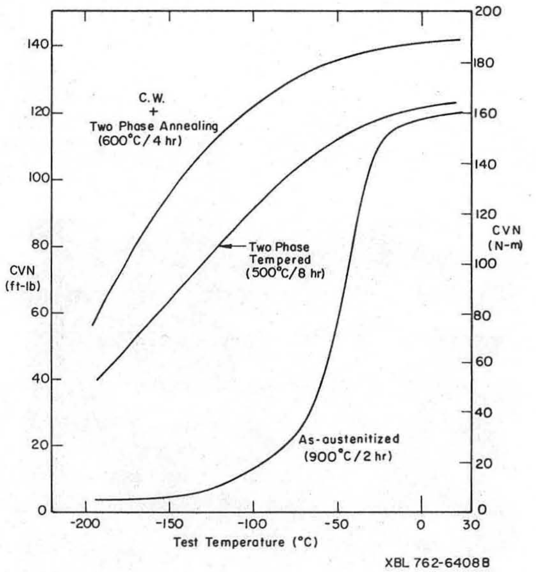
C.W.
+
Two Phase Annealing
(600°C/4 hr)
Two Phase
Tempered
(500°C/8 hr)
As-austenitized
(900°C/2 hr)
CVN
(ft-lb)
CVN
(N-m)
0
20
40
60
80
100
120
140
0
20
40
60
80
100
120
140
160
180
200
-200
-150
-100
-50
0
30
Test Temperature (°C)
XBL 762-64088

FIG. 2

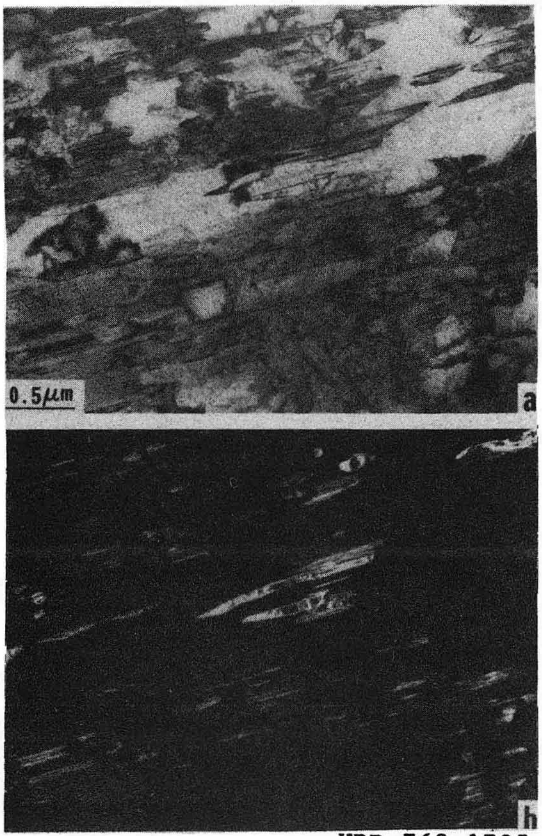

XBB 762-1735

FIG. 3

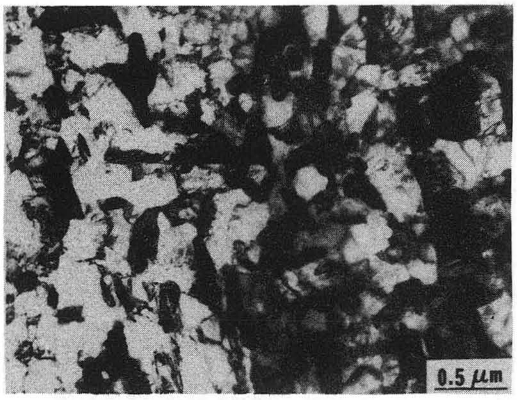

XBB 762-6723

FIG. 4

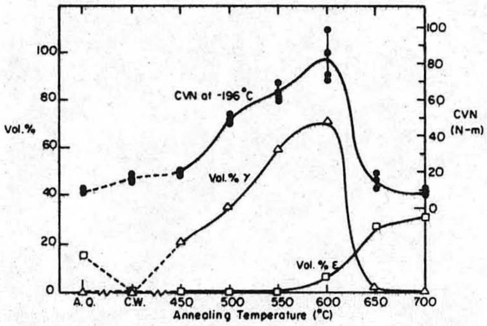

XBL 765-6824B

FIG. 5

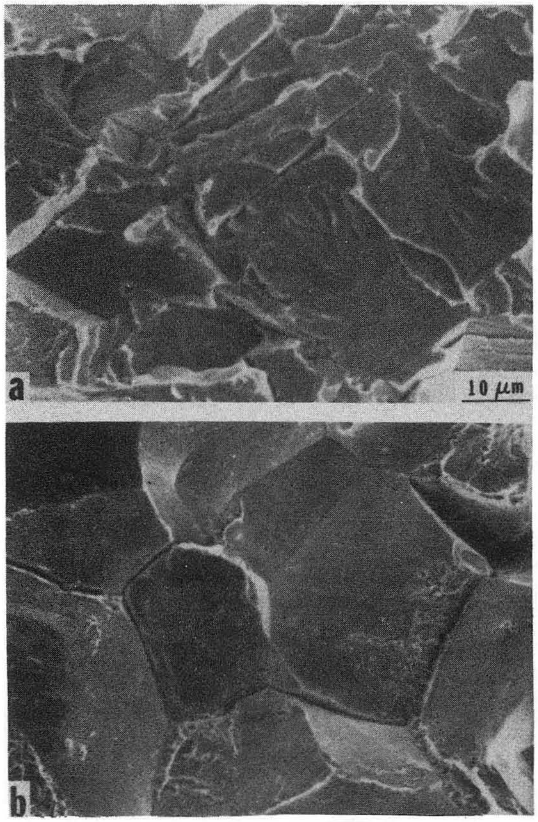

XBB 786-6721

FIG. 6

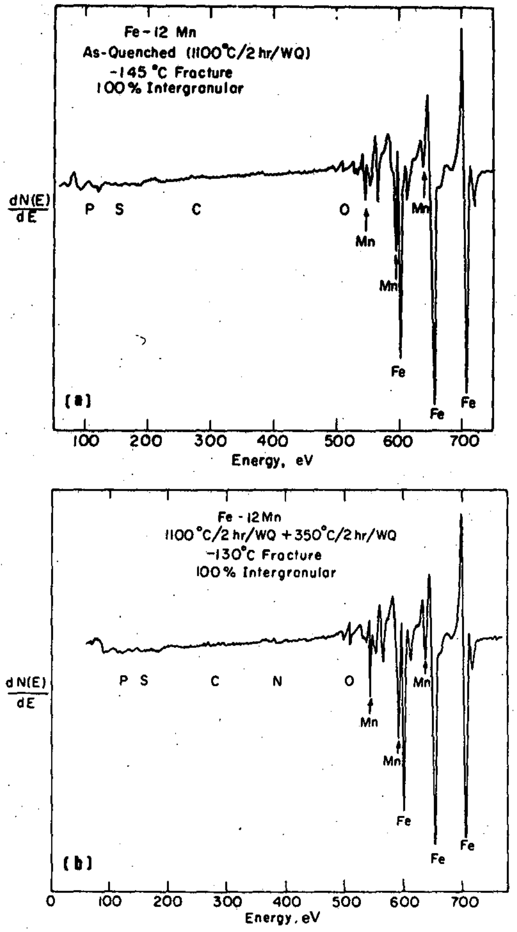

XBL 774-5351A

FIG. 7

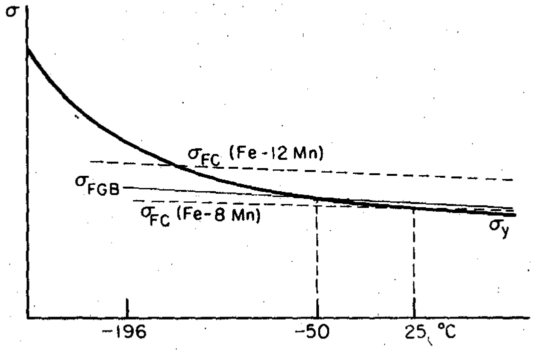

XBL 786-5211

FIG. 8

TECHNICAL INFORMATION DEPARTMENT
LAWRENCE BERKELEY LABORATORY
UNIVERSITY OF CALIFORNIA
BERKELEY, CALIFORNIA 94720